

■ **ARTHRITIS**

# Exosomes from dysfunctional chondrocytes affect osteoarthritis in Sprague-Dawley rats through FTO-dependent regulation of PIK3R5 mRNA stability

**G. Lv,  
B. Wang,  
L. Li,  
Y. Li,  
X. Li,  
H. He,  
L. Kuang**

From The Second Xiangya Hospital of Central South University, Changsha, China

**Aims**

Exosomes (exo) are involved in the progression of osteoarthritis (OA). This study aimed to investigate the function of dysfunctional chondrocyte-derived exo (DC-exo) on OA in rats and rat macrophages.

**Methods**

Rat-derived chondrocytes were isolated, and DCs induced with interleukin (IL)-1 $\beta$  were used for exo isolation. Rats with OA (n = 36) or macrophages were treated with DC-exo or phosphate-buffered saline (PBS). Macrophage polarization and autophagy, and degradation and chondrocyte activity of cartilage tissues, were examined. RNA sequencing was used to detect genes differentially expressed in DC-exo, followed by RNA pull-down and ribonucleo-protein immunoprecipitation (RIP). Long non-coding RNA osteoarthritis non-coding transcript (OANCT) and phosphoinositide-3-kinase regulatory subunit 5 (PIK3R5) were depleted in DC-exo-treated macrophages and OA rats, in order to observe macrophage polarization and cartilage degradation. The PI3K/AKT/mammalian target of rapamycin (mTOR) pathway activity in cells and tissues was measured using western blot.

**Results**

DC-exo inhibited macrophage autophagy (p = 0.002) and promoted M1 macrophage polarization (p = 0.002). DC-exo at 20  $\mu$ g/ml induced collagen degradation (p < 0.001) and inflammatory cell infiltration (p = 0.023) in rats. OANCT was elevated in DC (p < 0.001) and in cartilage tissues of OA patients (p < 0.001), and positively correlated with patients' Kellgren-Lawrence grade (p < 0.001). PIK3R5 was increased in DC-exo-treated cartilage tissues (p < 0.001), and OANCT bound to fat mass and obesity-associated protein (FTO) (p < 0.001). FTO bound to PIK3R5 (p < 0.001) to inhibit the stability of PIK3R5 messenger RNA (mRNA) (p < 0.001) and disrupt the PI3K/AKT/mTOR pathway (p < 0.001).

**Conclusion**

Exosomal OANCT from DC could bind to FTO protein, thereby maintaining the mRNA stability of PIK3R5, further activating the PI3K/AKT/mTOR pathway to exacerbate OA.

**Cite this article:** *Bone Joint Res* 2022;11(9):652–668.

**Keywords:** Osteoarthritis, Dysfunctional chondrocyte-derived exosomes, Long non-coding RNA OANCT, PIK3R5, FTO

**Article focus**

■ The regulatory function of dysfunctional chondrocyte-derived exosomes (DC-exo) on osteoarthritic (OA) rats and macrophages was investigated.

■ The underlying molecular mechanism of DC-exo in OA was explored.

Correspondence should be sent to Lei Kuang; email: lei.kuang@csu.edu.cn

doi: 10.1302/2046-3758.119.BJR-2021-0443.R2

*Bone Joint Res* 2022;11(9):652–668.

### Key messages

- DC-exo promote M1 macrophage polarization and exacerbate symptoms in OA rats.
- Significantly increased expression of long non-coding RNA osteoarthritis non-coding transcript (OANCT) is identified in DC-exo.
- OANCT binding to fat mass and obesity-associated protein regulates phosphoinositide-3-kinase regulatory subunit 5 (PIK3R5) mRNA stability.

### Strengths and limitations

- This study confirmed that DC-exo accentuated OA by enhancing M1-type polarization of macrophages and attenuating autophagy.
- A potential pitfall of this work may be the application of chondrocytes induced by interleukin-1 $\beta$ , which has been reported to show insignificant impact on OA in vivo as the source of exosomes.

### Introduction

Osteoarthritis (OA) remains the most prevalent degenerative joint condition and a leading cause of pain and disability in adults, whose aetiology includes joint injury, obesity, ageing, as well as heredity.<sup>1,2</sup> It has been noted that targeting the polarization of macrophages can suppress inflammation in the joints, thus relieving OA symptoms.<sup>3</sup> Macrophages can polarize to pro-inflammatory (M1) and anti-inflammatory (M2) phenotypes, and the latter is related to wound-healing by the production of arginase (Arg) and prochondrogenic cytokines, such as interleukin (IL)-10 and transforming growth factor- $\beta$  (TGF- $\beta$ ).<sup>4</sup> Therefore, determining the molecular mechanism of macrophage polarization could be important for the treatment of OA.

Exosomes (exo) are observed to change with OA progression, and multiple joint cells including chondrocytes, synovial fibroblasts, and osteoblasts can secrete exosomes that influence the biological effects of recipient cells.<sup>5</sup> Chondrocytes are the resident cells for articular cartilage, and the dysfunctional chondrocyte (DC) may severely cause the failure of articular cartilage.<sup>6</sup> Interestingly, chondrocyte-targeting exosomes could serve as vehicles for the delivery of microRNA-140 into chondrocytes, which might be a novel treatment of OA.<sup>7</sup> However, whether the cargoes of DC-derived exosomes (DC-exo) have direct repercussions on macrophage polarization remains largely unclear. A large number of long non-coding RNA (lncRNA) have been found to be differentially expressed in pathological processes of OA, including extracellular matrix (ECM) degradation, synovial inflammation, and chondrocyte apoptosis.<sup>8,9</sup> In the present study, by using high-throughput sequencing, we identified a novel lncRNA AC002091.2 which was significantly upregulated in chondrocytes treated with IL-1 $\beta$ , and named it lncRNA osteoarthritis

non-coding transcript (OANCT). In addition, its counterpart AC002091.1 is one of the top lncRNAs regulated by endotoxemia in monocytes, but not in adipose tissue.<sup>10</sup> N6-methyladenosine (m6A) is a dynamic methylation at the N6 site of adenosine. For lncRNAs, m6A modifications can both interact with m6A mediators to facilitate their function, and modulate RNA-protein interactions via RNA structural switches.<sup>11</sup> More importantly, m6A modification influences virtually all dynamic biological processes and molecular functions, and the abnormal m6A modification will inevitably cause a series of diseases, including OA.<sup>12</sup> In addition, fat mass and obesity-associated protein (FTO)-dependent demethylation of m6A controls mRNA splicing, and is necessary for adipogenesis.<sup>13</sup> In this study, through exploring the functional role of OANCT in DC-exo, we aimed to provide a new perspective for a better understanding of OA. Our study indicates that DC-exo can accentuate OA in rats and M1-polarization of macrophage through the delivery of OANCT. We determined whether exosomal OANCT affects macrophage polarization and cartilage degeneration during OA by regulating FTO-mediated m6A modification.

### Methods

**Subject enrolment.** The present study was authorized by the Ethics Committee of the the Second Xiangya Hospital of Central South University. All patients with OA and the normal controls who participated in the present study signed a written informed consent. A total of 53 cases of cartilage tissues from patients with varying degrees of OA, and 16 cases of normal cartilage tissues, were collected from 2016 to 2018. Normal knee cartilage tissues were from patients with post-traumatic amputations and femoral condylar fractures. These normal controls were free of osteophytes or joint space narrowing on radiograph, and without osteochondral deformity of the knee. OA cartilage tissues were categorized according to the Kellgren-Lawrence (KL)<sup>14</sup> grade. The Kellgren-Lawrence scoring system is a method for grading the severity of knee OA. According to knee radiographs, the patients were scored as grade 0 (normal knee), grade 1 (mild narrowing of the knee joint, i.e. cartilage wear), grade 2 (small osteophytes and narrowing of the joint space on radiograph), grade 3 (large amount of moderate osteophytes, narrowing of the joint space, or deformity of knee joint), and grade 4 (large amount of osteophytes on radiograph, severe narrowing of the joint space, and deformity of knee joint).

**Chondrocyte culture.** Knee cartilage tissues from eight-week-old rats (n = 6, 200 g (standard deviation (SD) 20), from Beijing Vital River Laboratory Animal Technology, China) were flushed twice with phosphate-buffered saline (PBS) and trimmed with a #11 sterile surgical blade on the surface of the specimen and at the edge of the abraded area. The specimen was rinsed again using PBS

and detached with 0.15% type II collagenase (diluted ten times) in the tube in a shaking table (37°C, 80 rpm) for four to six hours. The tubes were then centrifuged at 1,000 rpm for eight minutes, and the supernatant was discarded. The cells were then identified by light microscopy of the cell morphology and immunofluorescence of the chondrocyte marker collagen II in the cells.

After identification, chondrocytes were treated with IL-1 $\beta$  (50  $\mu$ g/ml, Sigma-Aldrich, USA). Changes in the expression of matrix metalloproteinase family (MMP1 and MMP9), and ECM-related proteins collagen II and aggrecan in chondrocytes, were detected by reverse transcription-quantitative (RT-q) polymerase chain reaction (PCR) and immunofluorescence.

**Extraction and identification of DC-exo.** DC-exo were extracted using a modified ultracentrifugation method. The cell culture medium after IL-1 $\beta$  induction was collected, and DC-exo were separated using Exoquick Reagent (System Biosciences, USA). The conditioned medium was incubated with Exoquick reagent (5:1) for more than 12 hours and centrifuged at 1,500  $\times$ g for 30 minutes. The precipitated exo were re-suspended in 100  $\mu$ l PBS and stored at -80°C. Nanosight LM10 particle tracking analysis, transmission electron microscopy (TEM), and western blot detection of exosome marker proteins CD63, CD9, CD81, and ALG-2 interacting protein X (ALIX) were used for DC-exo identification.

**OA rat modelling.** Animal experiments were reviewed and approved by the ethical review committee of the Second Xiangya Hospital of Central South University. A total of 42 Sprague-Dawley rats were randomly allocated into an OA group (n = 36) and a sham group (n = 6). After anaesthesia using intraperitoneal injection of ketamine hydrochloride (0.08 mg/100 g) and xylazine (0.04 mg/100 g), the right knee area was sterilized with alcohol. A 28-gauge needle was inserted perpendicularly to the inferior aspect of the patella, penetrated the patellar ligament, and turned proximally into the knee joint cavity until a sensation of subsidence was felt. Papain and L-cysteine were added to saline to make a 4% papain solution and 0.3 mol/l cysteine solution before use. The model rats were injected with the mixture of 4% (w/v) papain and 0.3 mol/l cysteine at 0.25 ml/kg into the right knee joint cavity.<sup>15</sup> Injections were given on days 1, 4, 7, 10, and 13. On the fifth day after the last papain injection (day 18), 20  $\mu$ g/ml DC-exo or an equivalent amount of PBS was administered into the knee joint. Injections were given every five days for four consecutive injections. The rats were euthanized at day 40 for a modified Mankin score.<sup>16</sup> The operation of the sham-operated group was the same as that of the model group, but an equal amount of saline was injected. Serum from rats was collected and frozen at -80°C for subsequent testing. Extended procedures can be found in the Supplementary Material. For all experiments involving animals, we have adhered to the ARRIVE guidelines and have supplied an ARRIVE checklist in the Supplementary Material.

**Macrophage culture and treatment.** Bone marrow-derived macrophages were produced from non-adherent bone marrow cell suspensions of rats from which chondrocytes were extracted. Bone marrow was flushed from the femur and tibia by centrifugation at 3,000  $\times$ g for five minutes in a microcentrifuge and cultured for four hours to remove differentiated macrophages. Non-adherent cells were counted, seeded at 0.375  $\times$  10<sup>6</sup> cells/ml in 96-well plates, and cultured with 0.2 ml Dulbecco's Modified Eagle Medium (DMEM) with 10% foetal bovine serum (FBS), 100 IU/ml penicillin/streptomycin and 20% L929. The cells were cultured for one week after changing the medium on day 3.

Macrophages in good growth condition were infected with lentiviruses to reduce the expression of OANCT or PIK3R5. The lentiviral (Lv) vectors containing short hairpin RNAs (shRNAs) were purchased from Shanghai GenePharma Bioengineering (China). Briefly, Lv-Enhance was first diluted in DMEM plus 10% FBS to obtain the appropriate Lv-Enhance (1  $\times$ ). Macrophages were seeded at 1  $\times$  10<sup>6</sup> cells/ml. After washing with PBS, the cells were cultured in medium containing Lv-Enhance (1  $\times$ ) and mixed with Lv vectors having a multiplicity of infection (MOI) of 30 to 50. To obtain effective infection, infected macrophages were kept growing for three days. If cell viability was impaired, culture media were replaced with fresh DMEM and promptly supplemented with 10% FBS. After examination under an inverted microscope, infection efficiency was verified by reverse transcription-quantitative polymerase chain reaction (RT-qPCR) and western blot.

**RT-qPCR.** Total RNA was extracted from the cells using the TRIzol method. RNA was extracted from cartilage tissues using RNeasy fibrous tissue kit (Qiagen company, Germany). In brief, the tissues were stabilized in RNA, later grounded with liquid nitrogen, and then lysed in lysis solution. After the addition of 70% ethanol and a centrifugation on RNeasy spin column with buffer, RNA pellet was obtained. Total RNA (1  $\mu$ g) was used for reverse transcription using a Primescript RT kit (Takara Bio, Japan) following the manufacturer's protocol. Real-time quantitative PCR was performed on a ViiA 7 real-time PCR system using SYBRPremix Ex Taq II (Takara Bio). Glyceraldehyde-3-phosphate dehydrogenase (GAPDH) was regarded as a reference gene. The PCR reaction experiment of each sample was repeated three times, and the RT-qPCR data were analyzed by the 2<sup>- $\Delta\Delta$ Ct</sup> method. The primer sequences of these targets are provided in Supplementary Table i. **Statistical analysis.** GraphPad Prism 6 (GraphPad Software, USA) software was used for data analysis. The data are reported as the mean and standard deviation (SD). The data in the present study were derived from more than three biologically independent experiments. Independent-samples *t*-test or one-way/two-way variance analysis (ANOVA) with Tukey's post hoc test was employed. Statistical significance was accepted for *p* < 0.05.

## Results

**DC-exo promote the polarization of M1 macrophages.** Under the light microscope, the isolated and cultured rat chondrocytes were small, mostly triangular or irregularly shaped, and highly shaded, resembling paving stone. We used immunofluorescence to detect the chondrocyte marker collagen II, and found that this was mainly localized in the cytoplasm (Supplementary Figure a). To mimic the OA-resembling environment, we added IL-1 $\beta$  to the chondrocyte medium. We found that after IL-1 $\beta$  treatment, the levels of MMP1 and MMP9 in chondrocytes were increased significantly, and aggrecan and collagen II accumulation was significantly reduced (Supplementary Figure a). Subsequently, we further extracted exosomes from PBS- or IL-1 $\beta$ -treated chondrocytes. The particle size of the extracted exosomes was analyzed using Nanosight LM10 particle tracking, and we found that the extracted exosomes were all in the range of 80 to 120 nm (Supplementary Figure a). Transmission electron microscope (TEM) revealed that the exosomes of chondrocytes had distinct ellipsoidal or barrel-like structures (Supplementary Figure a). We further verified the expression of the exosomal marker proteins CD63, CD9, CD81, and ALIX using western blot. CD63, CD9, CD81, and ALIX protein expression was found to be significantly higher in exosomes relative to chondrocytes (S1C-1:  $p < 0.001$ ; S1C-2:  $p = 0.002$ ; S1D-1:  $p < 0.001$ ; S1D-2:  $p = 0.001$ ; S1E-1:  $p < 0.001$ ; S1E-2:  $p = 0.002$ ; S1F-1:  $p < 0.001$ ; S1F-2:  $p < 0.001$ ; all independent-samples *t*-test), indicating that exosomes were successfully extracted (Supplementary Figure a).

Subsequently, we used exosomes from PBS-treated or different doses of IL-1 $\beta$ -treated chondrocytes, respectively, to treat the macrophages. As the dose of exosomes from IL-1 $\beta$ -treated chondrocytes increased, the proportion of macrophages polarized toward the M1 type was significantly increased (1a: PBS vs 10:  $p = 0.006$ , PBS vs 20:  $p < 0.001$ , PBS vs 40:  $p < 0.001$ ; 1b: PBS vs 10:  $p < 0.001$ ; PBS vs 20:  $p < 0.001$ ; PBS vs 40:  $p < 0.001$ , all one-way ANOVA) (Figures 1a and 1b). Exosomes from IL-1 $\beta$ -treated chondrocytes significantly promoted an inflammatory phenotype in macrophages, as evidenced by a significant increase in the levels of TNF- $\alpha$  (all  $p < 0.001$ ; one-way ANOVA), IL-12 (PBS vs 10:  $p = 0.001$ , PBS vs 20:  $p < 0.001$ , PBS vs 40:  $p < 0.001$ ; one-way ANOVA), and IL-6 (all  $p < 0.001$ ; one-way ANOVA), and a significant decrease in the level of IL-10 (PBS vs 10:  $p = 0.003$ , PBS vs 20:  $p < 0.001$ , PBS vs 40:  $p < 0.001$ ; one-way ANOVA) and TGF- $\beta$  (PBS vs 10:  $p = 0.001$ , PBS vs 20:  $p < 0.001$ , PBS vs 40:  $p < 0.001$ ; one-way ANOVA) (Figure 1c). Furthermore, the polarized phenotype of macrophages is closely linked to the modulation of autophagy, and decreased levels of autophagy in macrophages can promote their M1 polarization.<sup>17,18</sup> Thus, we used monodansylcadaverine (MDC) staining to detect the level of autophagy in macrophages, and we found that the level of autophagy in macrophages co-cultured with DC-exo was significantly reduced (PBS vs 10:

$p = 0.038$ , PBS vs 20:  $p = 0.003$ , PBS vs 40:  $p < 0.001$ ; one-way ANOVA) (Figure 1d). Furthermore, we examined the expression of autophagy-related genes Atg4B, p62, and Beclin-1 in macrophages and observed that co-culture with DC-exo significantly decreased the expression of Atg4B (1e: PBS vs 10:  $p = 0.030$ , PBS vs 20:  $p = 0.005$ , PBS vs 40:  $p < 0.001$ ; 1f: PBS vs 10:  $p = 0.006$ , PBS vs 20:  $p < 0.001$ , PBS vs 40:  $p < 0.001$ ; two-way ANOVA) and Beclin-1 (1e: PBS vs 10:  $p = 0.036$ , PBS vs 20:  $p = 0.006$ , PBS vs 40:  $p < 0.001$ ; 1f: PBS vs 10:  $p = 0.049$ , PBS vs 20:  $p = 0.006$ , PBS vs 40:  $p < 0.001$ ; two-way ANOVA) in macrophages (Figures 1e and 1f). Moreover, the proportion of LC3-positive particles in the cells was observed under a fluorescence microscope, and we found a significant decline in the number of positive cells in DC-exo-treated macrophages (Figure 1g). TEM was conducted to detect the formation of autophagic vesicles in the cells. The number of autophagic vesicles in the cytoplasm of DC-exo-treated macrophages was significantly reduced (Figure 1h), in which the cytoplasmic autophagosomes had a multilayered membrane structure.

**DC-exo exacerbate symptoms in rats with OA.** To investigate the effect of DC-exo on OA, we used papain injections into the rat knee joint cavity to construct a rat model of OA. Five days after model establishment, exosomes derived from PBS- or IL-1 $\beta$ -treated chondrocytes were injected intra-articularly at an interval of five days until the endpoint (Figure 2a). The OA in rats was evaluated using Mankin's modified score. It was found that OA symptoms were significantly exacerbated after DC-exo treatment (Figure 2b). The contents of pro-inflammatory factors were significantly increased (all  $p < 0.001$ ; one-way ANOVA), whereas those of anti-inflammatory factors were reduced, in the knee joint cavity of rats (Figure 2c). Subsequently, we extracted knee cartilage tissues from rats to detect the level of cartilage degradation in knee tissues using toluidine blue staining. The degradation of cartilage tissues from OA rats was aggravated after DC-exo treatment (Figure 2d). We further used haematoxylin and eosin (H&E) staining to observe the knee tissues of rats. The knee joints of rats with OA had more obvious damage and immune cell infiltration after DC-exo treatment (Figure 2e). We then used immunohistochemistry to detect a significant augment in the number of inducible nitric oxide synthase (iNOS)-positive cells (both  $p < 0.001$ ; one-way ANOVA) and a significant decline in the number of Arg-positive cells (both  $p < 0.001$ ; one-way ANOVA) in cartilage tissues (Figures 2f and 2g). The results of terminal deoxynucleotidyl transferase dUTP nick end labeling (TUNEL) assay showed an elevation (both  $p < 0.001$ ; one-way ANOVA) in the number of apoptotic cells in cartilage tissues after DC-exo treatment (Figure 2h). Finally, we measured the collagen content in rat cartilage tissues using a collagen deposition kit and observed that the collagen content in OA rat cartilage tissues was significantly reduced (both  $p < 0.001$ ; one-way ANOVA) after

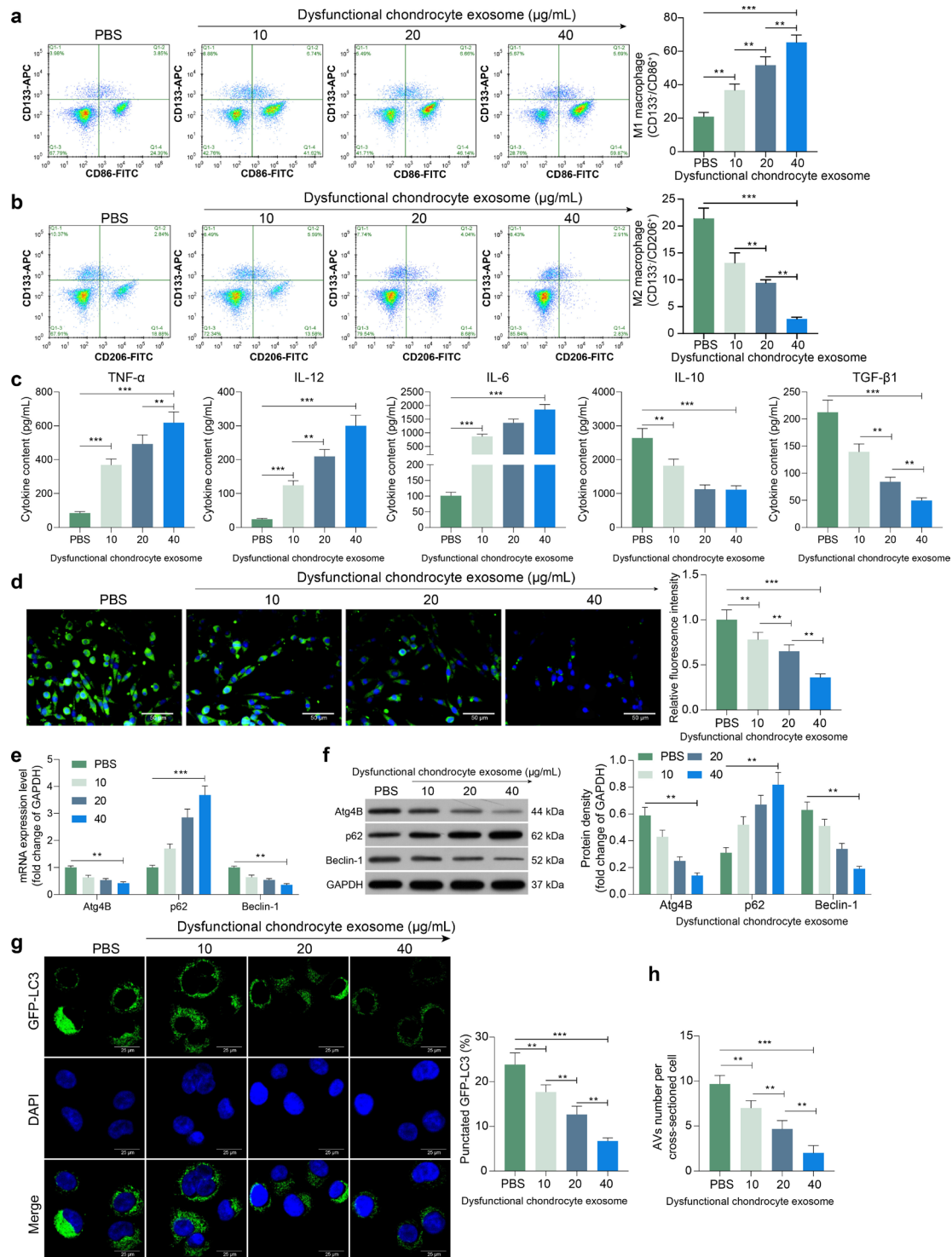


Fig. 1

Dysfunctional chondrocyte-derived exosomes (DC-exo) promote M1-type polarization of macrophages. a) Flow cytometry detection of macrophage M1 polarization (CD133/CD86<sup>+</sup>) and b) M2 polarization (CD133/CD206<sup>+</sup>). c) Enzyme-linked immunosorbent assay for the detection of inflammatory factors tumour necrosis factor alpha (TNF- $\alpha$ ), interleukin (IL)-12, IL-6, transforming growth factor beta (TGF- $\beta$ ), and IL-10 produced by macrophage culture. d) Changes in autophagy levels in macrophages evaluated by monodansylcadaverine staining. e) Reverse transcription-quantitative polymerase chain reaction and f) western blot detection of messenger RNA (mRNA) and protein expression of autophagy-related factors Atg4B, p62, and Beclin-1 in macrophages. g) Proportion of cells with LC3-positive granules in macrophages by fluorescence detection. h) transmission electron microscopy (TEM) observation of the formation of autophagic vesicles in macrophages. The results are representative of three independent experiments. All data are represented as mean and standard deviation, and analyzed using one-way or two-way analysis of variance with Tukey's post-test. \*\* $p < 0.01$ , \*\*\* $p < 0.001$ . AV, autophagic vesicles; DAPI, 4',6-diamidino-2-phenylindole; GAPDH, glyceraldehyde-3-phosphate dehydrogenase; GFP-LC3, green fluorescent protein-microtubule associated protein 1 light chain 3; PBS, phosphate-buffered saline.

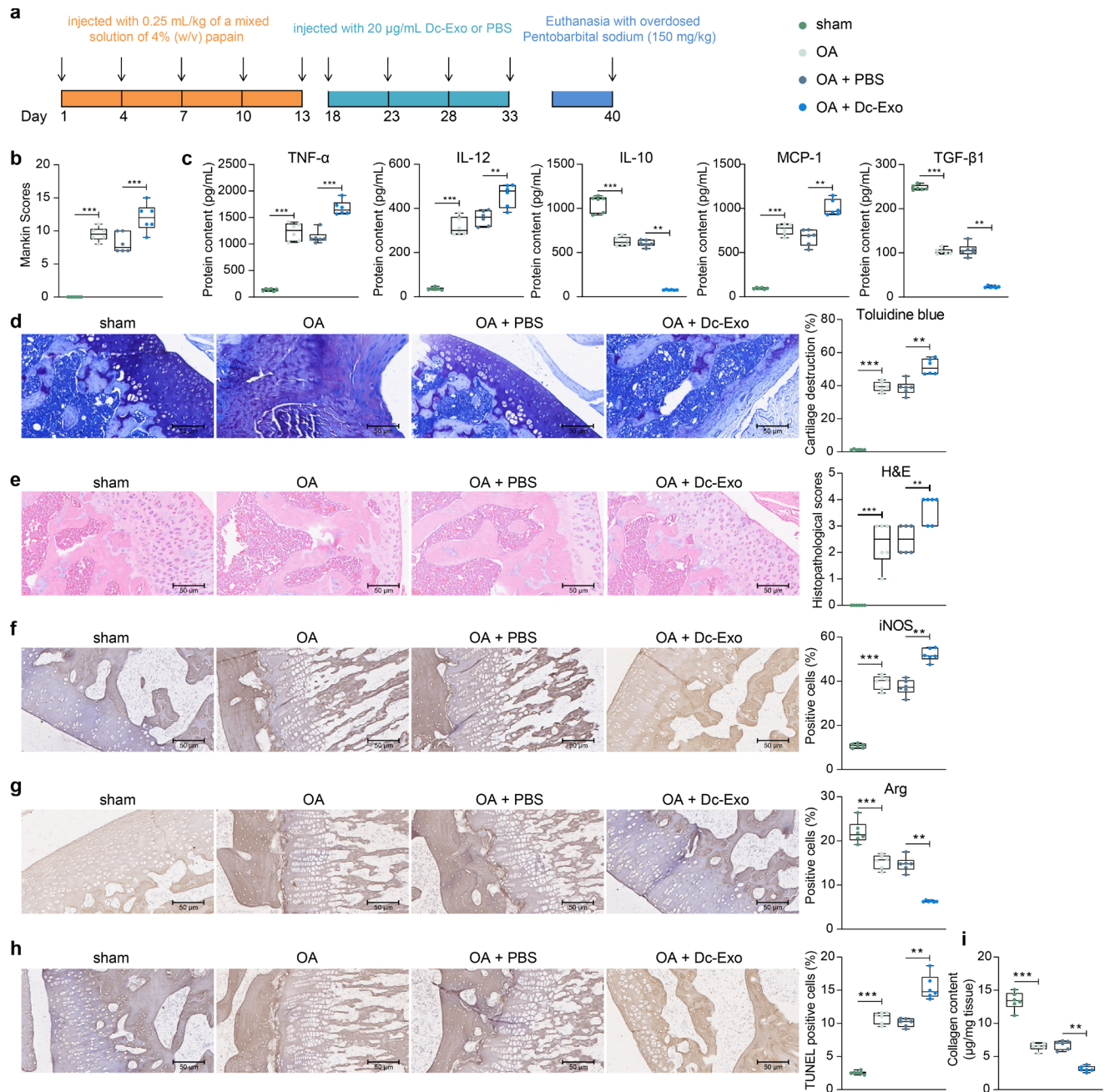


Fig. 2

Dysfunctional chondrocyte-derived exosomes (DC-exo) exacerbate symptoms in osteoarthritic (OA) rats. a) Schematic diagram of the rat modelling and interventions. b) Symptoms in rats assessed by Mankin score. c) Enzyme-linked immunosorbent assay for the detection of tumour necrosis factor alpha (TNF- $\alpha$ ), interleukin (IL-12), IL-10, monocyte chemoattractant protein-1 (MCP-1), and transforming growth factor beta (TGF- $\beta$ ) in rat knee joint fluid. d) Cartilage degradation in rats evaluated by toluidine blue staining. e) Pathologically damaged structures in rat knee assessed by haematoxylin and eosin staining. f) Positive cell rate of inducible nitric oxide synthase (iNOS) and g) arginine in rat knee tissues by immunohistochemical staining. h) Terminal deoxynucleotidyl transferase dUTP nick end labeling (TUNEL) assay detection of apoptosis in rat cartilage tissue. i) Collagen content in rat cartilage tissue assessed by the collagen deposition kit. Each group contains six rats, with each dot representing one rat. The results are representative of three independent experiments. All data are represented as mean and standard deviation, and analyzed using one-way analysis of variance with Tukey's post-test. \*\* $p < 0.01$ , \*\*\* $p < 0.001$ .

DC-exo administration (Figure 2i). These results suggest that the inflammatory conditions in OA lead to chondrocyte dysfunction, and that the secreted exosomes will promote M1-type macrophage polarization and further exacerbate the symptoms of OA.

**oANCT expression is significantly increased in DC-exo.** To investigate the molecular composition of DC-exo, we used high-throughput sequencing to analyze and identify the DC-exo collected. A new lncRNA-AC002091.2 with the highest expression was identified, which we

found to be consistent with AC002091.2 in the LncRNA database by DNAMAN comparison (6.0; LynnonBiosoft, Canada).<sup>19</sup> It was thus named Inc-OANCT (Figure 3a). Subsequently, we further verified the expression of OANCT in IL-1 $\beta$ -treated chondrocytes. RT-qPCR revealed that the expression of OANCT in IL-1 $\beta$ -treated chondrocytes and their exosomes was much higher (both  $p < 0.001$ ; independent-samples  $t$ -test) than that of PBS-treated chondrocytes (Figure 3b). Furthermore, we examined the expression and distribution of OANCT in chondrocytes and cartilage tissues of OA rats by fluorescence in situ hybridization (FISH) experiments, and we found that OANCT was distributed in both chondrocytes and cartilage tissues (Figures 3c and 3d). We then examined the expression of OANCT in macrophages after co-culture with exosomes, or in cartilage tissues of rats after exosome administration, and found that there was a significant upregulation in OANCT expression in macrophages (PBS vs 10:  $p = 0.008$ , PBS vs 20:  $p < 0.001$ , PBS vs 40:  $p < 0.001$ ; one-way ANOVA) or cartilage tissues (all  $p < 0.001$ ; one-way ANOVA) after exosomal treatment relative to their expression after PBS treatment. We further observed that the expression of OANCT in the knee tissues of OA rats was much higher than that of sham-operated rats (Figures 3e and 3f).

To further define the role of OANCT in the progression of OA, we clinically collected cartilage tissues from 53 OA patients and 16 non-OA patients who required meniscal arthroplasty due to fracture injury. We first examined the expression of OANCT by RT-qPCR and found that its expression was significantly higher (independent-samples  $t$ -test;  $p < 0.001$ ) in the cartilage tissues of OA patients than in those of normal controls (Figure 3g). Furthermore, we classified 53 patients with OA according to the KL classification, and found a positive correlation with the severity of OA with the expression of OANCT (one-way ANOVA; I vs II:  $p = 0.045$ , I vs III:  $p < 0.001$ , I vs IV:  $p < 0.001$ , II vs III:  $p < 0.001$ , II vs IV:  $p < 0.001$ , III vs IV:  $p = 0.003$ ) (Figure 3h).

**Knockdown of OANCT inhibits M1-type polarization of macrophages.** Based on our previous results, we believed that OANCT has a critical role in the progression of OA and the polarization of macrophages. To validate our conjecture, we transfected shRNA targeting OANCT in macrophages treated with DC-exo, and verified the transfection efficiency by RT-qPCR (one-way ANOVA; both  $p < 0.001$ ) (Figure 4a). Subsequently, we used flow cytometry to detect the proportions of polarized macrophages, and found a significant decline in the proportion of macrophages that were polarized toward M1 (shScr vs shONACT-#1:  $p = 0.016$ , shScr vs shONACT-#2:  $p = 0.006$ ; one-way ANOVA) and a significant elevation in the proportion of macrophages that were polarized toward M2 (both  $p < 0.001$ ; one-way ANOVA) after knocking down the expression of OANCT (Figures 4b and 4c). Consistently, the secretion of TNF- $\alpha$  (shScr vs shONACT-#1:  $p = 0.006$ , shScr vs shONACT-#2:  $p = 0.003$ ; one-way ANOVA), IL-12 (one-way ANOVA; shScr vs shONACT-#1:  $p = 0.018$ , shScr

vs shONACT-#2:  $p = 0.003$ ), and IL-6 (both  $p < 0.001$ ; one-way ANOVA) was significantly decreased, and IL-10 (shScr vs shONACT-#1:  $p = 0.006$ , shScr vs shONACT-#2:  $p = 0.002$ ; one-way ANOVA) and TGF- $\beta$ , both  $p < 0.001$ ; (one-way ANOVA) levels were significantly increased in macrophages after knocking down OANCT (Figure 4d). Additionally, changes in autophagy levels in macrophages were examined, and we found that knocking down OANCT further promoted autophagy in macrophages (Figures 4e to 4g).

In a previous study, it was shown that macrophages with different polarization types have different effects on the development of OA.<sup>3,20</sup> After co-culturing primary chondrocytes with macrophages, it was strikingly found that ECM degradation in chondrocytes was significantly reduced (4h, first graph: both  $p < 0.001$ ; 4h, second graph: shScr vs shONACT-#1:  $p = 0.002$ , shScr vs shONACT-#2:  $p < 0.001$ ; 4i, first graph: shScr vs shONACT-#1:  $p = 0.001$ , shScr vs shONACT-#2:  $p < 0.001$ ; 4i, second graph: shScr vs shONACT-#1:  $p = 0.010$ , shScr vs shONACT-#2:  $p = 0.006$ ; 4j, first graph: shScr vs shONACT-#1:  $p = 0.002$ , shScr vs shONACT-#2:  $p < 0.001$ ; 4j, second graph: shScr vs shONACT-#1:  $p = 0.007$ , shScr vs shONACT-#2:  $p = 0.002$ ; 4k, first graph: both  $p < 0.001$ ; 4k, second graph: shScr vs shONACT-#1:  $p < 0.002$ , shScr vs shONACT-#2:  $p < 0.001$ ; all one-way ANOVA) after co-culturing with macrophages with shOANCT, and the percentage of apoptosis was significantly reduced (shScr vs shONACT-#1:  $p = 0.002$ , shScr vs shONACT-#2:  $p < 0.001$ ; one-way ANOVA) (Figures 4h to 4l).

**Knockdown of OANCT relieves symptoms in rats with OA.** To further clarify the role of OANCT in the progression of OA, we injected shRNAs targeting OANCT into the knee joint cavity of rats treated with DC-exo (Figure 5a). We first detected a significant reduction (one-way ANOVA; both  $p < 0.001$ ) in the expression of OANCT in cartilage tissues using RT-qPCR (Figure 5b). Subsequently, we measured the levels of inflammatory factors in the knee joint cavity of rats using ELISA, and found that the inflammatory response in the knee joint was significantly reduced (TNF- $\alpha$ : both  $p < 0.001$ ; IL-12: shScr vs shONACT-#1:  $p = 0.027$ , shScr vs shONACT-#2:  $p = 0.006$ ; IL-10: both  $p < 0.001$ ; MCP-1: shScr vs shONACT-#1:  $p = 0.005$ , shScr vs shONACT-#2:  $p = 0.019$ ; TGF- $\beta$ : both  $p < 0.001$ ; all one-way ANOVA) after knocking down OANCT (Figure 5c). Toluidine blue staining and H&E staining further revealed that OANCT knockdown resulted in reduced cartilage degradation, pathologically damaged structures in knee cartilage tissues, and immune cell infiltration (Figures 5d and 5e). The results of immunohistochemistry exhibited a significant decline (shScr vs shONACT-#1:  $p = 0.022$ , shScr vs shONACT-#2:  $p = 0.002$ ; one-way ANOVA) in the number of iNOS-positive cells and a promotion in the number of Arg-positive cells in the cartilage tissues of rats harbouring OANCT knockdown (Figures 5f and 5g). In addition, we observed a significant decline (both  $p < 0.001$ ; one-way ANOVA) in the percentage of apoptosis in chondrocytes (Figure 5h). Knocking down OANCT

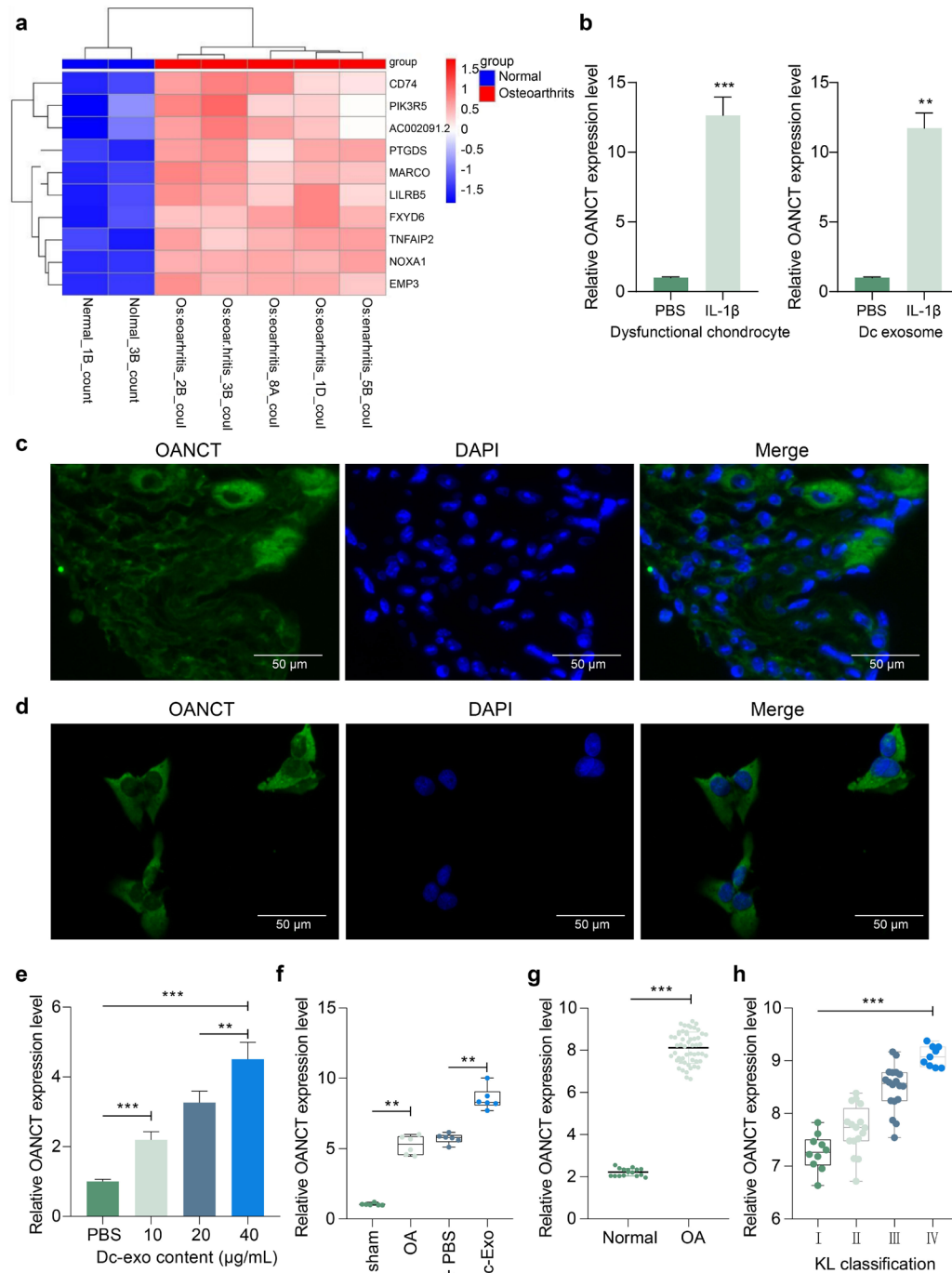


Fig. 3

The expression of osteoarthritis non-coding transcript (OANCT) is significantly increased in dysfunctional chondrocyte-derived exosomes (DC-exo). a) Heatmap of microarray screening of exosome from normal chondrocytes and interleukin beta (IL-1 $\beta$ )-treated chondrocytes. b) OANCT expression in chondrocytes and their exosomes detected by reverse transcription-quantitative polymerase chain reaction (RT-qPCR). c) Fluorescence in situ hybridization (FISH) assay to detect the expression and distribution of OANCT in cartilage tissues or d) chondrocytes. e) RT-qPCR for OANCT expression in exosome-treated macrophages or f) rat cartilage tissues. g) RT-qPCR detection of OANCT expression in knee tissues from 53 osteoarthritis (OA) patients and 16 non-OA patients requiring meniscal arthroplasty due to fracture injury. h) Spearman correlation analysis of the correlation between the expression of OANCT and the patients' Kellgren-Lawrence (KL) grade in 53 patients with OA. Each group contains six rats, with each dot representing one rat. The results are representative of three independent experiments. All data are represented as mean and standard deviation and analyzed using independent-samples *t*-test, and one-way analysis of variance with Tukey's post-test. \*\**p* < 0.01, \*\*\**p* < 0.001. DAPI, 4',6-diamidino-2-phenylindole; EMP3, epithelial membrane protein 3; FXYD6, FXYD domain containing ion transport regulator 6; LILRB5, leucocyte immunoglobulin like receptor B5; MARCO, macrophage receptor with collagenous structure; NOXA1, NADPH oxidase activator 1; PBS, phosphate-buffered saline; PIK3R5, phosphoinositide-3-kinase regulatory subunit 5; PTGDS, prostaglandin D2 synthase; TNFAIP2, TNF alpha induced protein 2.

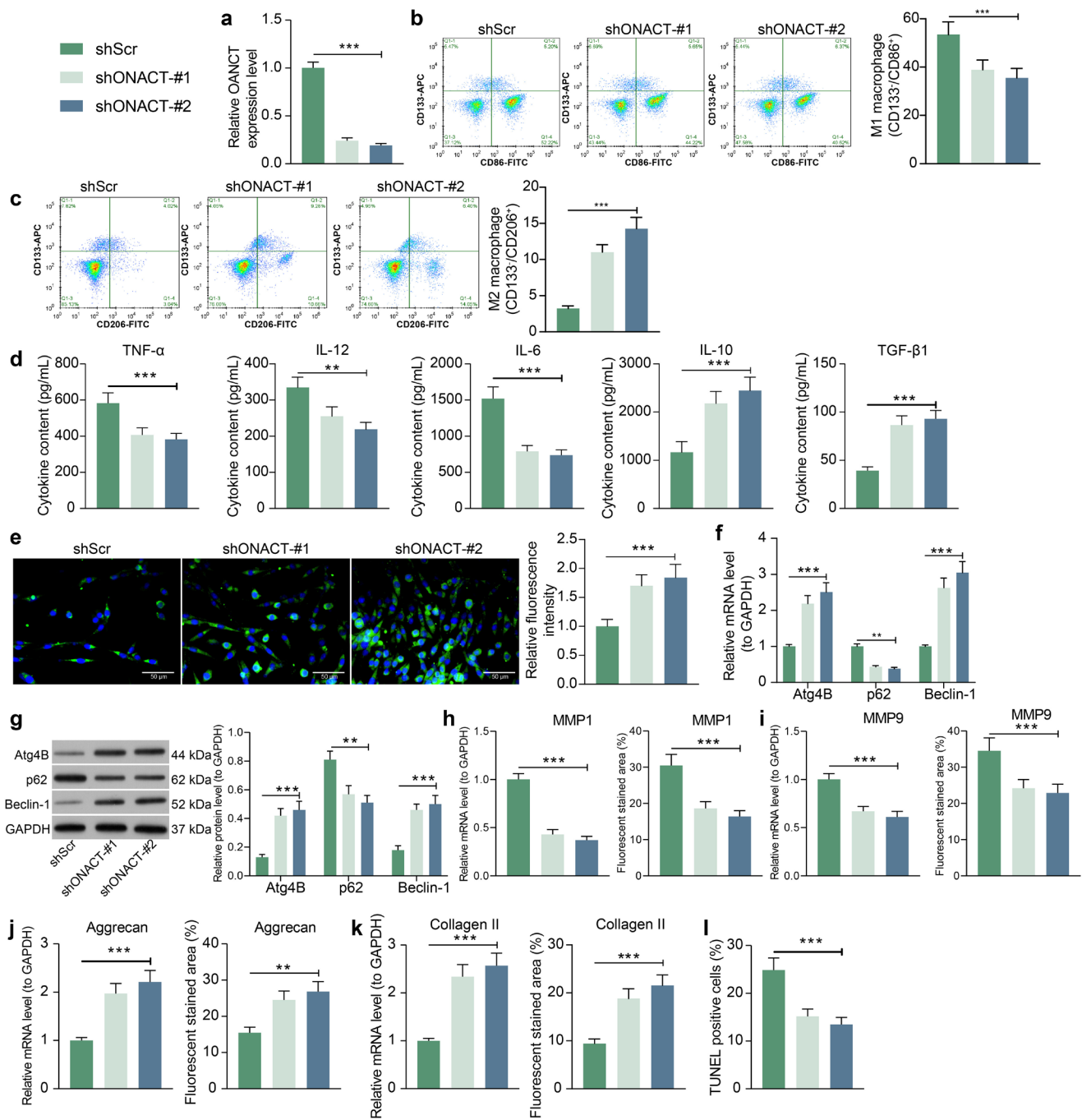


Fig. 4

Knockdown of osteoarthritis non-coding transcript (OANCT) inhibits M1-type polarization of macrophages. Macrophages co-cultured with dysfunctional chondrocyte-derived exosomes (DC-exo) were infected with short hairpin (sh)RNAs targeting OANCT. a) Expression of OANCT in macrophages detected by reverse transcription-quantitative polymerase chain reaction (RT-qPCR). b) Flow cytometry detection of macrophage M1 polarization (CD133/CD86<sup>+</sup>) and c) M2 polarization (CD133/CD206<sup>+</sup>). d) Enzyme-linked immunosorbent assay for the detection of inflammatory factors tumour necrosis factor alpha (TNF- $\alpha$ ), interleukin (IL)-12, IL-6, transforming growth factor beta (TGF- $\beta$ ), and IL-10 produced by macrophage culture. e) Changes in autophagy levels in macrophages evaluated by monodansylcadaverine staining. f) RT-qPCR and g) western blot detection of messenger RNA (mRNA) and protein expression of autophagy-related factors Atg4B, p62, and Beclin-1 in macrophages. h) to k) Expression of: h) matrix metalloproteinase (MMP)1; i) MMP9; j) aggrecan; and k) collagen II in chondrocytes by RT-qPCR and immunofluorescence. l) Terminal deoxynucleotidyl transferase dUTP nick end labeling (TUNEL) assay of the level of apoptosis in chondrocytes. The results are representative of three independent experiments. All data are represented as mean and standard deviation, and analyzed using one-way or two-way analysis of variance with Tukey's post-test. \*\*p < 0.01, \*\*\*p < 0.001. GAPDH, glyceraldehyde-3-phosphate dehydrogenase.

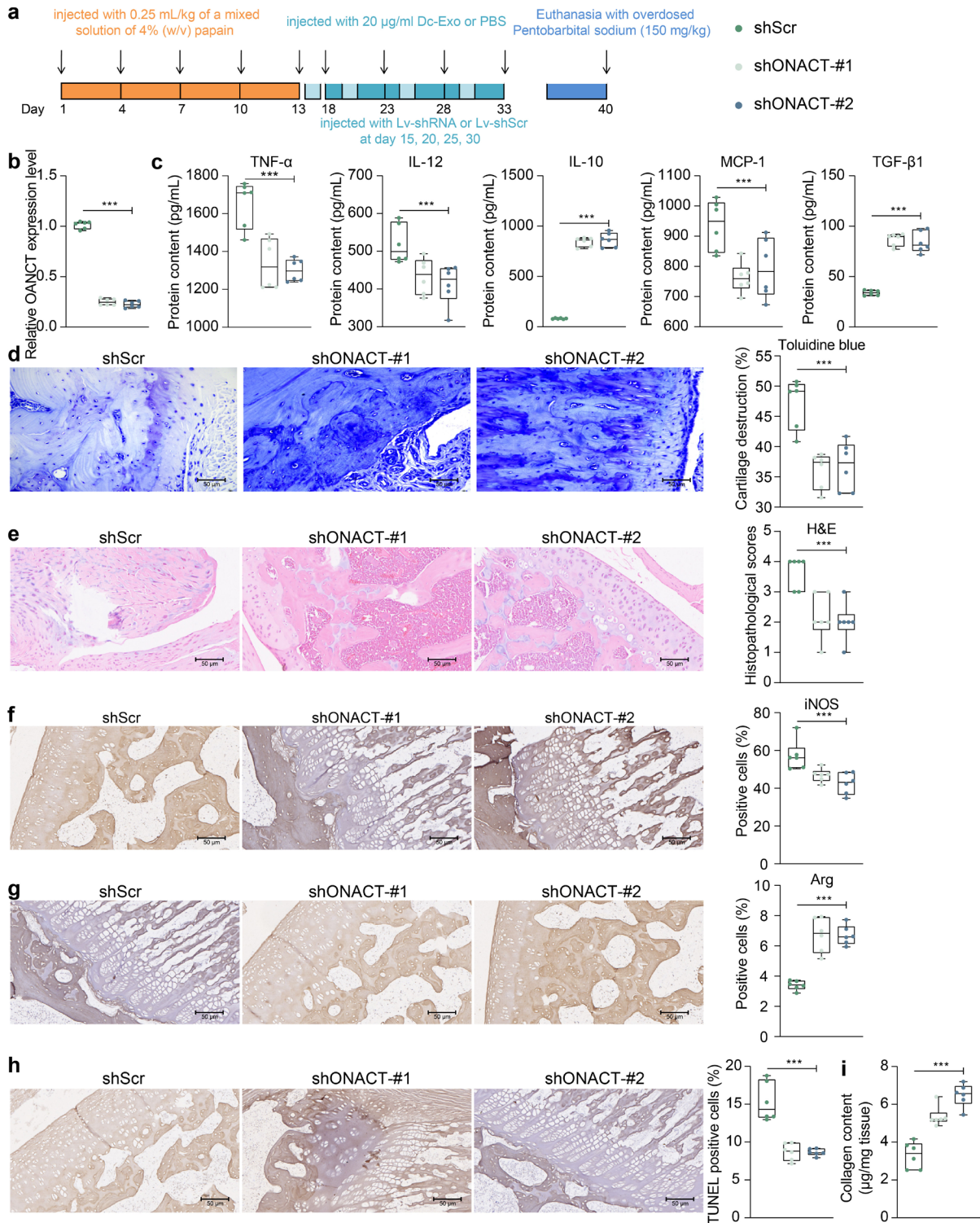


Fig. 5

Knockdown of osteoarthritis non-coding transcript (OANCT) alleviates symptoms in osteoarthritic (OA) rats. **a**) Schematic diagram of the rat modelling and interventions. **b**) Expression of OANCT in rat knee tissue by reverse transcription-quantitative polymerase chain reaction (RT-qPCR). **c**) Enzyme-linked immunosorbent assay for the detection of tumour necrosis factor alpha (TNF- $\alpha$ ), interleukin (IL)-12, IL-10, monocyte chemoattractant protein-1 (MCP-1), and transforming growth factor beta (TGF- $\beta$ ) in rat knee joint fluid. **d**) Cartilage degradation in rats evaluated by toluidine blue staining. **e**) Pathologically damaged structures in rat knee assessed by haematoxylin and eosin staining. **f**) Positive cell rate of inducible nitric oxide synthase (iNOS) and **g**) arginine in rat knee tissues by immunohistochemical staining. **h**) Terminal deoxynucleotidyl transferase dUTP nick end labeling (TUNEL) assay detection of apoptosis in rat cartilage tissue. **i**) Collagen content in rat cartilage tissue assessed by the collagen deposition kit. Each group contains six rats, with each dot representing one rat. The results are representative of three independent experiments. All data are represented as mean and standard deviation and analyzed using one-way analysis of variance with Tukey's post-test. \*\*\* $p < 0.001$ . ShScr, small hairpin RNA-scramble.

significantly reduced the collagen deposition degradation caused by DC-exo (both  $p < 0.001$ ; one-way ANOVA) (Figure 5i).

**OANCT regulates PIK3R5 mRNA stability by binding to the FTO protein.** Our previous unpublished studies have revealed that OANCT could bind to the FTO protein. We found that OANCT was expressed in the cytoplasm and nucleus (green fluorescence), while FTO was mainly expressed in the cytoplasm (red fluorescence). OANCT and FTO co-localized in cartilage tissues and cells (Figures 6a and 6b). Subsequently, we further employed RNA pull-down and RIP experiments to verify whether OANCT could bind to the FTO protein. The level of FTO enrichment was significantly increased in macrophages over-expressing OANCT (Figures 6c and 6d), indicating that OANCT can bind to the FTO protein in macrophages. To further investigate the binding sites of OANCT to FTO, we constructed a series of partially deleted OANCT mutants. The results show that OANCT $\Delta$ 2 had the closest binding relation with FTO (Figures 6e and 6f), suggesting that the sequence located on the OANCT nucleotide 636 to 1,272 bp acts as a major site for FTO binding. Insignificant changes in FTO mRNA expression were found following knockdown of OANCT in macrophages (Figure 6g).

To explore the downstream signalling pathways of OANCT, we further used RNA-seq high-throughput sequencing to analyze differentially expressed genes and enriched signalling pathways in cartilage tissues of DC-exo-treated OA rats. The autophagy inhibitory pathway PI3K/AKT/mammalian target of rapamycin (mTOR)-related genes were upregulated, with the PI3K receptor PIK3R5 showing the highest correlation with OANCT expression (Figures 6h and 6i). We further analyzed the clinically collected cases and found that the expression of PIK3R5 was significantly higher ( $p < 0.001$ ; independent-samples *t*-test) in the cartilage tissues of OA patients than in non-OA patients (Figure 6j). The expression of PIK3R5 was positively correlated with the expression of OANCT and with the KL grade (I vs II:  $p = 0.043$ , I vs III:  $p < 0.001$ , I vs IV:  $p < 0.001$ , II vs III:  $p = 0.0234$ , II vs IV:  $p < 0.001$ , III vs IV:  $p = 0.045$ ; one-way ANOVA) (Figures 6k and 6l). Moreover, the expression of PIK3R5 increased significantly (all  $p < 0.001$ ; one-way ANOVA) after DC-exo treatment in both cartilage tissues and macrophages, but decreased significantly (all  $p < 0.001$ ; one-way ANOVA) after further knockdown of OANCT (Figures 6m and 6n). We verified the mRNA half-life of PIK3R5 by treating macrophages infected with shOANCT or shScr, separately with the actinomycin D, a RNA synthesis inhibitor. It was found that the degradation rate of PIK3R5 in macrophages with OANCT knockdown was significantly higher (6 h: shScr vs shOANCT-#1:  $p = 0.006$ , shScr vs shOANCT-#2:  $p < 0.001$ ; for the other timepoints and groups: all  $p < 0.001$ ; two-way ANOVA) than that in macrophages with shScr (Figure 6o).

**OANCT activates the PI3K/AKT/mTOR pathway by regulating the mRNA stability of PIK3R5 in a m6A-dependent manner.** In a study by Panoutsopoulou et al,<sup>21</sup> a

correlation was found between FTO expression and the development of rheumatoid arthritis or OA. Since FTO acts as an eraser of m6A, we speculated that the stability of PIK3R5 mRNA was maintained due to the binding of OANCT to FTO, which reduced the demethylation modification of PIK3R5 mRNA by FTO. Therefore, we first predicted the m6A modification sites of PIK3R5 mRNA through the SRAMP website.<sup>22</sup> A total of six m6A modification sites were noted with very high confidence (Figures 7a and 7b). Therefore, we tested the binding relationship between FTO and PIK3R5 mRNA by RIP experiments, and found that FTO could bind significantly to the 1,201 to 1,245 bp segment of PIK3R5 mRNA ( $p < 0.001$ ; independent-samples *t*-test; Figure 7c). Therefore, we used methylated RNA immunoprecipitation (MeRIP)-qPCR to detect the level of m6A modification of PIK3R5 mRNA in macrophages. We found significant m6A modification at this site, but further treatment with DC-exo resulted in a further increase in m6A modification. Still, a significant decrease in m6A modification was noted after knockdown of OANCT expression (all  $p < 0.001$ ; one-way ANOVA; Figure 7d). The above results indicated that OANCT reduced the demethylation modification of the m6A sites of PIK3R5 by FTO binding, thereby maintaining the mRNA stability of PIK3R5.

Based on our prediction of RNA-seq high-throughput sequencing, we found that the autophagy-associated PI3K/AKT/mTOR signalling pathway was activated in DC-exo-treated rat cartilage tissues. The activation of the PI3K/AKT/mTOR signalling pathway in rat knee tissue was significantly activated by papain treatment and further promoted by DC-exo treatment, but the extents of the PI3K (all  $p < 0.001$ ; two-way ANOVA), AKT1 (all  $p < 0.001$ ; two-way ANOVA), and mTOR phosphorylation (sham vs OA:  $p < 0.001$ , PBS vs Dc-exo:  $p < 0.001$ , Dc-exo + shScr vs Dc-exo + shOANCT-#1:  $p < 0.001$ , Dc-exo + shScr vs Dc-exo + shOANCT-#1:  $p = 0.003$ , Dc-exo + shScr vs shOANCT-#2:  $p < 0.001$ ; two-way ANOVA) were significantly downregulated by shOANCT (Figure 7e). Similarly, the PI3K/AKT/mTOR signalling pathway was significantly activated in DC-exo-treated macrophages, but levels of phosphorylated PI3K, AKT1, and mTOR were significantly reduced after knockdown of OANCT expression (all  $p < 0.001$ ; two-way ANOVA; Figure 7f).

**Knockdown of PIK3R5 inhibits DC-exo-promoted M1 macrophage polarization.** In Figures 3 to 7, we found that exosomal OANCT from DC exacerbated the symptoms of OA by binding to FTO and inhibiting the ability of FTO of demethylation, thereby maintaining the mRNA stability of PIK3R5 and further promoting M1-type polarization of macrophages. Thus, to investigate the effects of PIK3R5 on macrophage polarization and autophagy, we further transfected shRNAs targeting PIK3R5 in DC-exo-treated macrophages and verified the transfection efficiency by RT-qPCR (both  $p < 0.001$ ; one-way ANOVA) and western blot (all  $p < 0.001$ ; two-way ANOVA) (Figures 8a and 8b). We found that the PI3K/AKT/mTOR signalling pathway in cells was also significantly blocked after knockdown

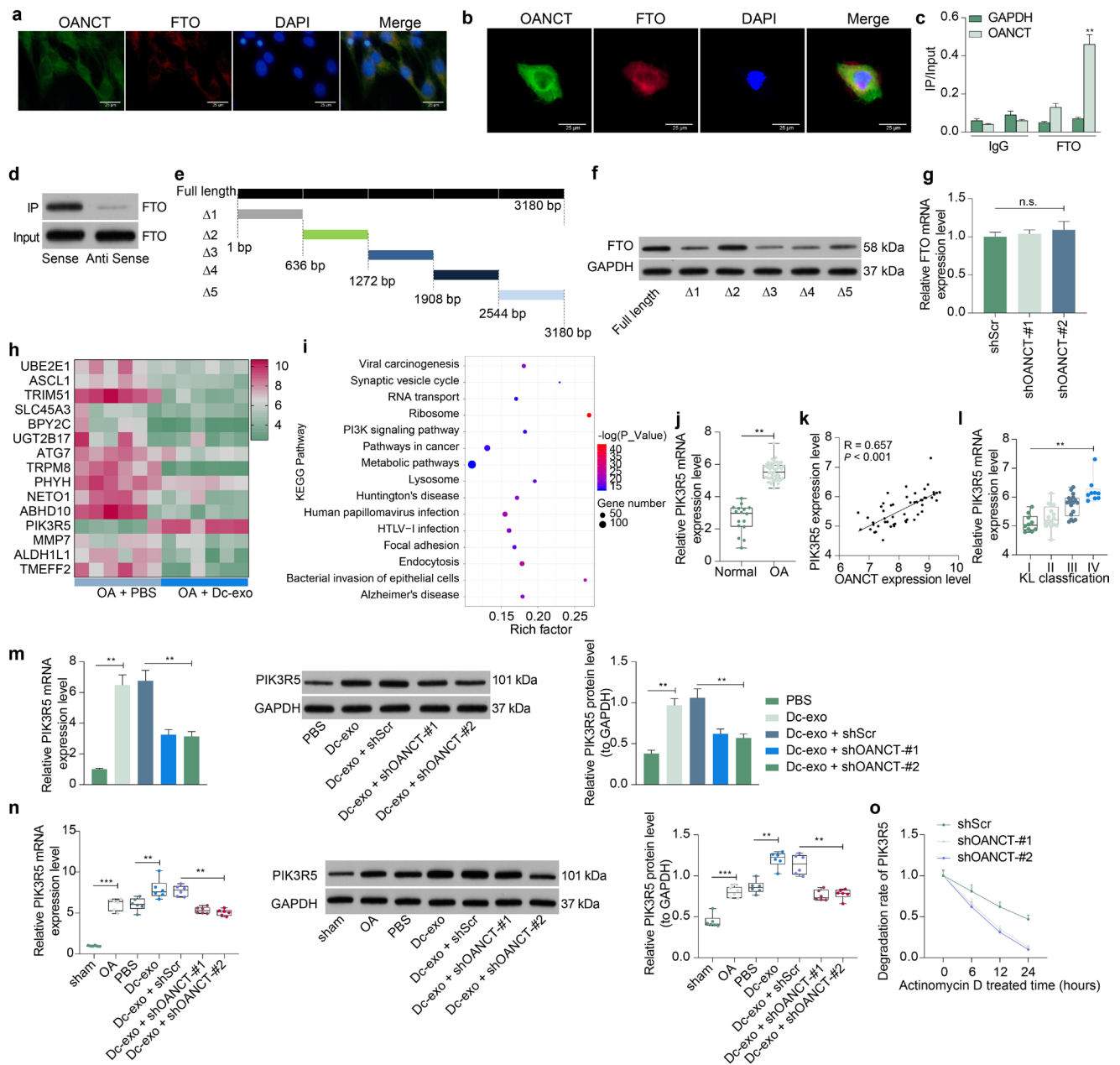


Fig. 6

Osteoarthritis non-coding transcript (OANCT) regulates phosphoinositide-3-kinase regulatory subunit 5 (PIK3R5) messenger RNA (mRNA) stability by binding to fat mass and obesity-associated protein (FTO). a) The localization of OANCT and FTO protein in rat cartilage tissues or b) chondrocytes detected by double-labelled fluorescence. c) The binding relation between OANCT and FTO protein examined by RNA pull-down and d) ribonucleoprotein immunoprecipitation (RIP) assays. e) Construction of OANCT sequences with different deletions. f) FTO protein levels bound to different mutant forms of OANCT detected by RNA pull-down assay. g) Changes in FTO mRNA expression after knockdown of OANCT in macrophages. h) Differentially expressed genes and i) enriched signalling pathways in cartilage tissues of dysfunctional chondrocyte-derived exosomes (DC-exo)-treated osteoarthritis (OA) rats analyzed by RNA-seq high-throughput sequencing. j) Phosphoinositide-3-kinase regulatory subunit 5 (PIK3R5) expression in knee tissues from 53 OA and 16 non-OA patients requiring meniscal arthroplasty due to fracture injury examined by reverse transcription-quantitative polymerase chain reaction (RT-qPCR). k) Spearman correlation analysis of the correlation between the expression of PIK3R5 and the expression of OANCT or l) the Kellgren-Lawrence grade in 53 patients with OA. m) RT-qPCR and western blot for mRNA and protein expression of PIK3R5 in chondrocytes or n) rat cartilage tissues. o) The expression of PIK3R5 mRNA in macrophages transfected with shOANCT and treated with IZCC-3 at different timepoints, as examined by RT-qPCR. The results are representative of three independent experiments. All data are represented as mean and standard deviation, and analyzed using independent-samples *t*-test, and one-way or two-way analysis of variance with Tukey's post-test. \*\**p* < 0.01, \*\*\**p* < 0.001. DAPI, 4',6-diamidino-2-phenylindole; GAPDH, glyceraldehyde-3-phosphate dehydrogenase; HTLV, human T-cell lymphotropic virus type 1; IgG, immunoglobulin G; IP, immunoprecipitation; KEGG, Kyoto Encyclopedia of Genes and Genomes; MMP, matrix metalloproteinase; PBS, phosphate-buffered saline; ShScr, small hairpin RNA-scramble.

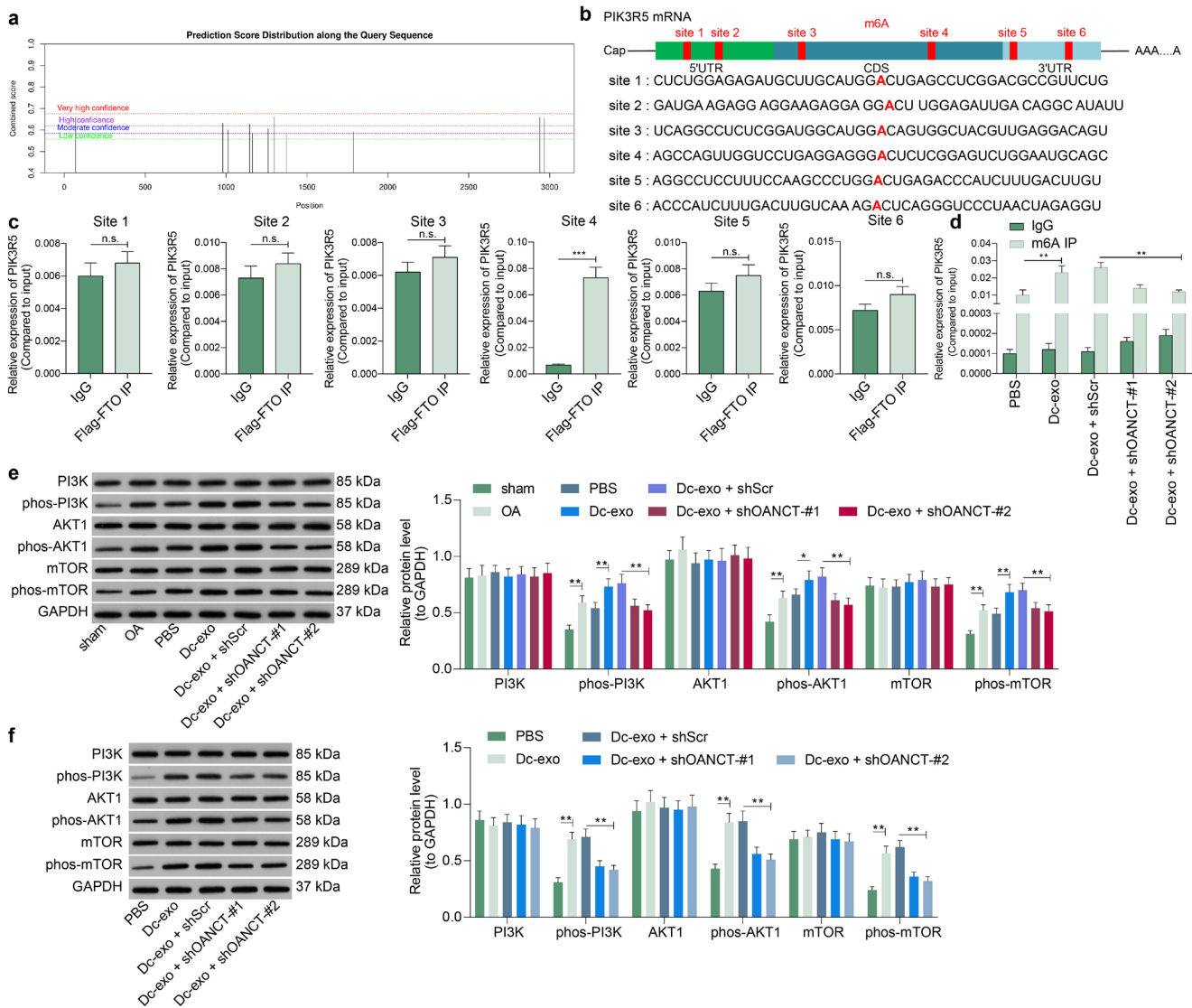


Fig. 7

Osteoarthritis non-coding transcript (OANCT) regulates the messenger RNA (mRNA) stability of phosphoinositide-3-kinase regulatory subunit 5 (PIK3R5) in a N6-methyladenosine (m6A)-dependent manner. a) Possible m6A modification sites for PIK3R5 mRNA predicted by the SRAMP website.<sup>22</sup> b) m6A sites with high confidence. c) The binding of fat mass and obesity-associated protein (FTO) to PIK3R5 mRNA validated by ribonucleoprotein immunoprecipitation (RIP). d) FTO-mediated demethylation of modified m6A on PIK3R5 mRNA verified by MeRIP-quantitative polymerase chain reaction (qPCR). e) Extent of PI3K, AKT serine/threonine kinase 1 (AKT1), and mammalian target of rapamycin (mTOR) phosphorylation in rat cartilage tissues and f) macrophages. The results are representative of three independent experiments. All data are represented as mean and standard deviation, and analyzed using independent-samples *t*-test, and one-way or two-way analysis of variance with Tukey's post-test. \*\**p* < 0.01. CDS, coding sequence; DC-exo, dysfunctional chondrocyte-derived exosomes; GAPDH, glyceraldehyde-3-phosphate dehydrogenase; IgG, immunoglobulin G; OA, osteoarthritis; PBS, phosphate-buffered saline; UTR, untranslated region.

of PIK3R5 (all *p* < 0.001; Figure 8b). Furthermore, our analysis revealed that after knockdown of PIK3R5, the proportion of macrophages with M1-type polarization decreased significantly (both *p* < 0.001; one-way ANOVA), whereas the proportion of M2-type polarization increased significantly (both *p* < 0.001; one-way ANOVA; Figures 8c and 8d). In addition, knocking down the expression of PIK3R5 further inhibited the secretion of pro-inflammatory cytokines in macrophages (TNF- $\alpha$ : shScr vs shPIK3R5-#1: *p* = 0.002, shScr vs shPIK3R5-#2: *p* < 0.001; IL-12: shScr vs shPIK3R5-#1: *p* = 0.004, shScr vs shPIK3R5-#2: *p* = 0.002; IL-6: shScr vs shPIK3R5-#1: *p* = 0.002, shScr vs shPIK3R5-#2: *p* = 0.001; one-way

ANOVA), whereas the levels of the anti-inflammatory cytokines IL-10 (shScr vs shPIK3R5-#1: *p* = 0.025, shScr vs shPIK3R5-#2: *p* = 0.016; one-way ANOVA) and TGF- $\beta$ 1 (both *p* < 0.001; one-way ANOVA) were significantly increased (Figure 8e). We then used MDC staining to detect the level of autophagy in macrophages. In the presence of shPIK3R5, the level of autophagy in macrophages was significantly enhanced (both *p* < 0.001; one-way ANOVA), which occurred concomitant with decreased expression of p62 (Figure 8g: shScr vs shPIK3R5-#1: *p* = 0.004, shScr vs shPIK3R5-#2: *p* = 0.003; Figure 8h: both *p* < 0.001; two-way ANOVA) and increased expression of Atg4B (all *p* < 0.001; two-way ANOVA) and Beclin-1

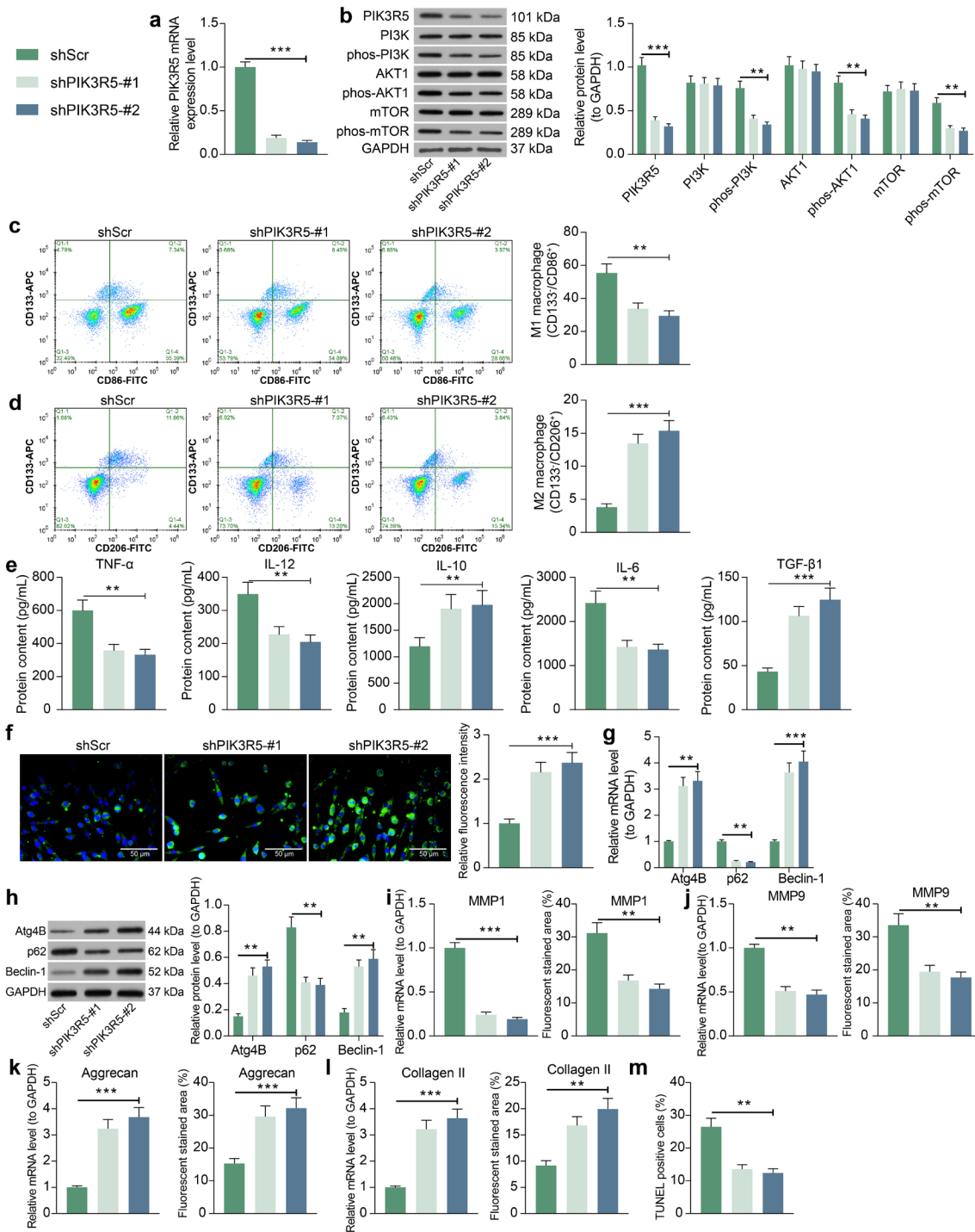


Fig. 8

Knockdown of phosphoinositide-3-kinase regulatory subunit 5 (PIK3R5) inhibits dysfunctional chondrocyte-derived exosomes (DC-exo)-promoted macrophage M1 polarization. Macrophages co-cultured with DC-exo were infected with short hairpin (sh)RNAs targeting PIK3R5. a) Expression of PIK3R5 in macrophages detected by reverse transcription-quantitative polymerase chain reaction (RT-qPCR). b) PIK3R5 protein and PI3K, AKT serine/threonine kinase 1 (AKT1), and mammalian target of rapamycin (mTOR) phosphorylation levels in macrophages detected by western blot. c) Flow cytometry detection of macrophage M1 polarization (CD133<sup>+</sup>/CD86<sup>+</sup>) and d) M2 polarization (CD133<sup>+</sup>/CD206<sup>+</sup>). e) Enzyme-linked immunosorbent assay (ELISA) for the detection of inflammatory factors tumour necrosis factor alpha (TNF- $\alpha$ ), interleukin (IL)-12, IL-6, transforming growth factor beta (TGF- $\beta$ ), and IL-10 produced by macrophage culture. f) Changes in autophagy levels in macrophages evaluated by monodansylcadaverine (MDC) staining. g) RT-qPCR and h) western blot detection of messenger RNA (mRNA) and protein expression of autophagy-related factors Atg4B, p62, and Beclin-1 in macrophages. i) to l) Expression of: i) matrix metalloproteinase (MMP)1; j) MMP9; k) aggrecan; and l) collagen II in chondrocytes by RT-qPCR and immunofluorescence. m) Terminal deoxynucleotidyl transferase dUTP nick end labeling (TUNEL) assay of the level of apoptosis in chondrocytes. The results are representative of three independent experiments. All data are represented as mean and standard deviation. Data were analyzed using one-way or two-way analysis of variance with Tukey's post-test. \*\*p < 0.01, \*\*\*p < 0.001. GAPDH, glyceraldehyde-3-phosphate dehydrogenase; ShScr, small hairpin RNA-scramble.

(all  $p < 0.001$ ; two-way ANOVA) (Figures 8f to 8h). Furthermore, after co-culturing chondrocytes with macrophages with shPIK3R5, the level of collagen deposition in chondrocytes increased significantly ((Figure 8i to 8k): all  $p < 0.001$ ; shScr vs shPIK3R5-#1:  $p = 0.002$ , shScr vs shPIK3R5-#2:  $p < 0.001$ ; Figure 8l: both  $p < 0.001$ ; shScr vs shPIK3R5-#1:  $p = 0.003$ , shScr vs shPIK3R5-#2:  $p < 0.001$ ; all one-way ANOVA) (Figures 8i to 8l) and the level of apoptosis in chondrocytes decreased significantly (both  $p < 0.001$ ; one-way ANOVA; Figure 8m).

## Discussion

Numbers of lncRNAs are dysregulated in OA cartilage, and some lncRNAs have been shown to participate in a large repertoire of pathological processes during OA, including ECM degradation, inflammatory responses, and apoptosis.<sup>23</sup> Meanwhile, the advent of exosomes as natural carriers of RNAs and proteins has raised great interest, as they may have the potential to harness these vesicles for delivery of miRNAs, mRNAs, and lncRNAs.<sup>24,25</sup> This study confirmed that DC-exo accentuated OA in a rat papain-induced model by enhancing M1-type polarization of macrophages and attenuating autophagy. We also demonstrated that expression of a novel lncRNA, OANCT, was promoted in OA via high-throughput sequencing technology of chondrocytes treated with IL-1 $\beta$ ; the knockdown of OANCT abrogated the effect of DC-exo on macrophages and OA rats by interacting with the FTO protein. Further analysis demonstrated that OANCT regulated the mRNA stability of PIK3R5 through an m6A-dependent way to mediate the PI3K/AKT/mTOR pathway.

Recently, Ragni et al<sup>26</sup> revealed that cytokines/chemokines and microRNAs conveyed within extracellular vesicles from adipose-derived mesenchymal stem cells can reduce ECM and switch an M1 inflammatory polarization of macrophages towards an M2 phenotype. By contrast, synovial fluid-derived exosomes appreciably stimulated the release of inflammatory cytokines, chemokines, and MMPs by M1 macrophages.<sup>27</sup> Likewise, the exosome-like vesicles from OA chondrocytes stimulated IL-1 $\beta$  secretion of macrophages and aggravated synovitis in OA.<sup>28</sup> All these findings have connected the function of exosomes with macrophage polarization. Moreover, impaired macrophage autophagy promotes the immune response in obese mice by driving proinflammatory macrophage polarization.<sup>17</sup> In our study, exosomes released by IL-1 $\beta$ -induced DC were found to expedite inflammatory response and prevent macrophages from autophagy *in vitro*. Our further *in vivo* evidence showed that DC-exo encouraged ECM degradation and apoptosis in OA rats. In addition, knockdown of exo-shuttled lnc-PVT1 alleviated lipopolysaccharide-induced OA progression.<sup>29</sup> Therefore, we postulated that the abovementioned function of DC-exo in OA was also elicited through the cargo of a lncRNA.

High-throughput sequencing technology enabled us to identify a novel lncRNA OANCT in OA. After

determining the presence of OANCT in cartilage tissues, we found that it was elevated in OA patients and positively correlated with KL grade. To substantiate the regulatory function of OANCT, we knocked down its expression via shRNAs in macrophages or OA rats pre-treated with DC-exo. As expected, OANCT silencing flattened the effects of DC-exo by evoking M2 phenotype switch and autophagy, and also reduced ECM accumulation both *in vitro* and *in vivo*. On the basis of a series of experiments, including double-labelled fluorescence, RNA pull-down, and RIP assays, it is fair to say that OANCT binds to the FTO protein.

FTO, also termed as ALKBH9, is the first identified m6A demethylase on mRNAs and has been indicated to be linked to increased OA risk through regulating BMI.<sup>21,30</sup> It has been suggested that rs8044769 in the FTO gene is not associated with OA susceptibility or higher BMI in the Chinese Han population.<sup>31,32</sup> In the present study, we also noticed that the FTO mRNA expression was not altered upon knockdown of OANCT in macrophages, further evidencing its role as a m6A demethylase in OA. More importantly, m6A modifications in mRNA/lncRNA play an important part in cellular energy homeostasis through their impact on the spliced mRNA/lncRNA populations.<sup>33</sup> Mechanistically, the exogenously overexpressed FTO binds to m6A motif-containing RNA sites, and FTO overexpression specifically removed m6A modification from GGACU and RRACU motifs in a concentration-mediated fashion.<sup>34</sup> However, the specific role of FTO and the underlying mechanism of action remains largely unclear. Our following RNA-seq high-throughput sequencing predicted the PI3K/AKT/mTOR pathway and the related receptor PIK3R5 as the most relevant effectors in OA. The PI3K/AKT signalling pathway has been identified as a common pathway for hip OA.<sup>35</sup> After the confirmation of the upregulation of PIK3R5 in OA patients, its direct binding relation with the FTO protein was substantiated in this study. Our subsequent MeRIP-qPCR further presented that OANCT maintained the mRNA stability of PIK3R5 by binding to FTO and reducing the demethylation modification of the m6A site of PIK3R5 by FTO. The close correlation between PIK3R5 and autophagy, as well as the AKT/mTOR signalling pathway, has been highlighted in osteosarcoma.<sup>36</sup> However, the linkage between PIK3R5 and inflammatory response has not been clearly characterized. Our final rescue experiments showed that shRNAs targeting PIK3R5 ameliorated the effects of DC-exo on macrophage polarization and OA progression as well.

In conclusion, we demonstrated that lncRNA OANCT, shuttled by DC-exo, significantly aggravated OA by inducing M1 macrophage polarization and reducing macrophage autophagy. Our data clearly illustrated that the potential of targeting shOANCT as a novel promising approach for OA was achieved through the FTO/PIK3R5/PI3K/AKT/mTOR axis (Supplementary Figure b). A potential pitfall of this work may be the application of chondrocytes induced by IL-1 $\beta$ , which has been reported to

show insignificant impact on OA in vivo,<sup>37</sup> as the source of exosomes. Therefore, the use of exosomes carrying OANCT from human OA chondrocytes, and from the cartilage of animals with mechanically induced OA, would be important in increasing our understanding of the involvement of OANCT in Dc-exo.

### Supplementary material



Extended procedures, the primer sequences for reverse transcription-quantitative polymerase chain reaction, the results for the identification of dysfunctional chondrocyte exosomes, and the mechanism diagram. An ARRIVE checklist is also included to show that the ARRIVE guidelines were adhered to in this study.

### References

- Eitner A, Wildemann B. Diabetes - osteoarthritis and joint pain. *Bone Joint Res.* 2021;10(5):307–309.
- Wang J, Zhou L, Zhang Y, Huang L, Shi Q. Mesenchymal stem cells - a promising strategy for treating knee osteoarthritis. *Bone Joint Res.* 2020;9(10):719–728.
- Sun Y, Zuo Z, Kuang Y. An emerging target in the battle against osteoarthritis: macrophage polarization. *Int J Mol Sci.* 2020;21(22):22.
- Fernandes TL, Gomoll AH, Lattermann C, Hernandez AJ, Bueno DF, Amano MT. Macrophage: a potential target on cartilage regeneration. *Front Immunol.* 2020;11:1111.
- Im GI. Current status of regenerative medicine in osteoarthritis. *Bone Joint Res.* 2021;10(2):134–136.
- Zhang H, Li J, Xiang X, et al. Tert-butylhydroquinone attenuates osteoarthritis by protecting chondrocytes and inhibiting macrophage polarization. *Bone Joint Res.* 2021;10(11):704–713.
- Liang Y, Xu X, Li X, et al. Chondrocyte-targeted microRNA delivery by engineered exosomes toward a cell-free osteoarthritis therapy. *ACS Appl Mater Interfaces.* 2020;12(33):36938–36947.
- Chen H, Chen L. An integrated analysis of the competing endogenous RNA network and co-expression network revealed seven hub long non-coding RNAs in osteoarthritis. *Bone Joint Res.* 2020;9(3):90–98.
- He CP, Jiang XC, Chen C, et al. The function of lncRNAs in the pathogenesis of osteoarthritis. *Bone Joint Res.* 2021;10(2):122–133.
- Ferguson JF, Xue C, Gao Y, et al. Tissue-specific differential expression of novel genes and long intergenic noncoding RNAs in humans with extreme response to evoked endotoxemia. *Circ Genom Precis Med.* 2018;11(11):e001907.
- Li X, Xiong X, Yi C. Epitranscriptome sequencing technologies: decoding RNA modifications. *Nat Methods.* 2016;14(1):23–31.
- Chen J, Tian Y, Zhang Q, et al. Novel insights into the role of N6-methyladenosine RNA modification in bone pathophysiology. *Stem Cells Dev.* 2021;30(1):17–28.
- Zhao X, Yang Y, Sun B-F, et al. FTO-dependent demethylation of N6-methyladenosine regulates mRNA splicing and is required for adipogenesis. *Cell Res.* 2014;24(12):1403–1419.
- KELLGREN JH, LAWRENCE JS. Radiological assessment of osteo-arthrosis. *Ann Rheum Dis.* 1957;16(4):494–502.
- Yang M, Chen C, Wang K, Chen Y, Xia J. Astilbin influences the progression of osteoarthritis in rats by down-regulation of PGE-2 expression via the NF- $\kappa$ B pathway. *Ann Transl Med.* 2020;8(12):766.
- Katsara O, Kolupaeva V. mTOR-mediated inactivation of 4E-BP1, an inhibitor of translation, precedes cartilage degeneration in rat osteoarthritic knees. *J Orthop Res.* 2018;36(10):2728–2735.
- Liu K, Zhao E, Ilyas G, et al. Impaired macrophage autophagy increases the immune response in obese mice by promoting proinflammatory macrophage polarization. *Autophagy.* 2015;11(2):271–284.
- Sergin I, Evans TD, Zhang X, et al. Exploiting macrophage autophagy-lysosomal biogenesis as a therapy for atherosclerosis. *Nat Commun.* 2017;8:15750.
- No authors listed. Transcript: lnc-NTN1-2.1. LNCipedia. <https://lncipedia.org/db/transcript/lnc-NTN1-2:1> (date last accessed 9 August 2022).
- Xue J, Chen J, Shen Q, et al. Addition of high molecular weight hyaluronic acid to fibroblast-like stromal cells modulates endogenous hyaluronic acid metabolism and enhances proteolytic processing and secretion of versican. *Cells.* 2020;9(7):E1681.
- Panoutsopoulou K, Metrustry S, Doherty SA, et al. The effect of FTO variation on increased osteoarthritis risk is mediated through body mass index: a Mendelian randomisation study. *Ann Rheum Dis.* 2014;73(12):2082–2086.
- No authors listed. SRAMP: A sequence-based N6-methyladenosine (m6A) modification site predictor. Cui Lab. 2016. <http://www.cuilab.cn/sramp/> (date last accessed 9 August 2022).
- Chen W-K, Yu X-H, Yang W, et al. lncRNAs: novel players in intervertebral disc degeneration and osteoarthritis. *Cell Prolif.* 2017;50(1):e12313.
- Barile L, Vassalli G. Exosomes: Therapy delivery tools and biomarkers of diseases. *Pharmacol Ther.* 2017;174:63–78.
- Tkach M, Théry C. Communication by extracellular vesicles: where we are and where we need to go. *Cell.* 2016;164(6):1226–1232.
- Ragni E, Perucca Orfei C, De Luca P, Colombini A, Viganò M, de Girolamo L. Secreted factors and EV-miRNAs orchestrate the healing capacity of adipose mesenchymal stem cells for the treatment of knee osteoarthritis. *Int J Mol Sci.* 2020;21(5):E1582.
- Domenis R, Zanutel R, Caponnetto F, et al. Characterization of the proinflammatory profile of synovial fluid-derived exosomes of patients with osteoarthritis. *Mediators Inflamm.* 2017;2017:4814987.
- Ni Z, Kuang L, Chen H, et al. The exosome-like vesicles from osteoarthritic chondrocyte enhanced mature IL-1 $\beta$  production of macrophages and aggravated synovitis in osteoarthritis. *Cell Death Dis.* 2019;10(7):522.
- Meng Y, Qiu S, Sun L, Zuo J. Knockdown of exosome-mediated lnc-PVT1 alleviates lipopolysaccharide-induced osteoarthritis progression by mediating the HMGB1/TLR4/NF- $\kappa$ B pathway via miR-93-5p. *Mol Med Rep.* 2020;22(6):5313–5325.
- Zhou Y, Kong Y, Fan W, et al. Principles of RNA methylation and their implications for biology and medicine. *Biomed Pharmacother.* 2020;131:110731.
- Dai J, Ying P, Shi D, et al. FTO variant is not associated with osteoarthritis in the Chinese Han population: replication study for a genome-wide association study identified risk loci. *J Orthop Surg Res.* 2018;13(1):65.
- Wang Y, Chu M, Rong J, et al. No association of the single nucleotide polymorphism rs8044769 in the fat mass and obesity-associated gene with knee osteoarthritis risk and body mass index: A population-based study in China. *Bone Joint Res.* 2016;5(5):169–174.
- Pan T. N6-methyl-adenosine modification in messenger and long non-coding RNA. *Trends Biochem Sci.* 2013;38(4):204–209.
- Li Y, Wu K, Quan W, et al. The dynamics of FTO binding and demethylation from the m(6)A motifs. *RNA Biol.* 2019;16(9):1179–1189.
- Qi X, Yu F, Wen Y, et al. Integration of transcriptome-wide association study and messenger RNA expression profile to identify genes associated with osteoarthritis. *Bone Joint Res.* 2020;9(3):130–138.
- Liu W, Jiang D, Gong F, et al. miR-210-5p promotes epithelial-mesenchymal transition by inhibiting PIK3R5 thereby activating oncogenic autophagy in osteosarcoma cells. *Cell Death Dis.* 2020;11(2):93.
- Nasi S, Ea HK, So A, Busso N. Revisiting the role of interleukin-1 pathway in osteoarthritis: interleukin-1 $\alpha$  and -1 $\beta$ , and NLRP3 inflammasome are not involved in the pathological features of the murine meniscectomy model of osteoarthritis. *Front Pharmacol.* 2017;8:282.

#### Author information:

- G. Lv, MD, Professor
  - B. Wang, MD, Professor
  - L. Li, MD, Orthopaedic Surgeon
  - Y. Li, MD, Orthopaedic Surgeon
  - X. Li, MD, Orthopaedic Surgeon
  - H. He, MD, Orthopaedic Surgeon
  - L. Kuang, MD, Orthopaedic Surgeon
- Department of Spine Surgery, The Second Xiangya Hospital of Central South University, Changsha, China.

#### Author contributions:

- G. Lv: Investigation, Formal analysis, Data curation, Writing – original draft.
- B. Wang: Writing – review & editing, Data curation.
- L. Li: Conceptualization, Data curation, Writing – review & editing.
- Y. Li: Methodology, Data curation, Writing – review & editing.
- X. Li: Resources, Data curation, Writing – review & editing.
- H. He: Methodology, Formal analysis, Data curation.
- L. Kuang: Methodology, Resources, Data curation.

#### Funding statement:

- The authors disclose receipt of the following financial or material support for the research, authorship, and/or publication of this article: this research was supported

by project funding from the Scientific research project of Hunan Provincial Health Commission (No. 202204073380).

**ICMJE COI statement:**

- All authors declare no conflicts of interest.

**Data sharing:**

- The datasets generated and/or analyzed during the current study are not publicly available due to the research design, but are available from the corresponding author on reasonable request.

**Ethical review statement:**

- The present study was authorized by the Ethics Committee of the Second Xiangya Hospital of Central South University. All patients with osteoarthritis (OA) and the normal controls who participated in the present study signed a written informed consent. Animal experiments were reviewed and approved by the ethical review committee of the Second Xiangya Hospital of Central South University and were per-

formed in compliance with the National Institute of Health's Guidelines of Laboratory Animal Care and Use in Biomedical Research. The ARRIVE checklist was also completed to show that ARRIVE guidelines were adhered to in this study.

**Open access funding**

- The open access fee for this study was covered by the Hunan Provincial Health Commission funding mentioned above.

© 2022 Author(s) et al. This is an open-access article distributed under the terms of the Creative Commons Attribution Non-Commercial No Derivatives (CC BY-NC-ND 4.0) licence, which permits the copying and redistribution of the work only, and provided the original author and source are credited. See <https://creativecommons.org/licenses/by-nc-nd/4.0/>